

Dinuclear uranyl coordination compound: Structural investigations and selective fluorescence sensing properties



Mohammad Azam ^{a,*}, Saud I. Al-Resayes ^a, Agata Trzesowska-Kruszynska ^b, Rafal Kruszynski ^b, Saikh Mohammad Wabaidur ^a, Saied M. Soliman ^c, Ranjan K. Mohapatra ^d, Mohammad Rizwan Khan ^a

^a Department of Chemistry, College of Science, King Saud University, P. O. Box 2455, Riyadh 11451, Saudi Arabia

^b Institute of General and Ecological Chemistry, Lodz University of Technology, Zeromskiego 116, 90-924 Lodz, Poland

^c Department of Chemistry, Faculty of Science, Alexandria University, P. O. Box 426, Ibrahimia, Alexandria 21321, Egypt

^d Department of Chemistry, Government College of Engineering, Keonjhar, Odisha 758002, India

ARTICLE INFO

Article history:

Received 29 May 2020

Accepted 3 August 2020

Available online 14 August 2020

Keywords:

Dinuclear uranyl coordination compound

Crystal structure

DFT studies

Sensing properties

ABSTRACT

The presence of Pb(II) ions and antibiotics in water beyond the permissible limits are among the leading factors causing water pollution. Therefore, their identification is quite necessary. In this article, we are concerned with a new dinuclear uranyl coordination compound holding a 1,3-bis(2-oxy-3-methoxybenzylidene)propan-2-olate moiety, in which each uranyl ion is seven coordinated. To obtain additional insights into the structure, DFT analyses were performed. Furthermore, Hirshfeld surface analysis was also recorded to determine the various intermolecular interactions in the studied coordination compound. The studied dinuclear uranyl coordination compound exhibited excellent fluorescence properties in water making it a promising candidate for sensing Pb(II) ions and antibiotics. The results suggest the studied compound has a high sensitivity for Pb(II) ions and the antibiotic Cefuroxime, with detection limits of 44.7 and 175 nM, respectively.

© 2020 Elsevier Ltd. All rights reserved.

1. Introduction

Uranium, isolated from pitchblende as uranium oxide, is a very important element used in nuclear fuel, weapons and fission power plants [1,2]. In addition, uranium has a variety of oxidation states. However, +VI is the only oxidation state stable under aerobic conditions, in the form of the uranyl(VI) cation UO_2^{2+} [3–5]. Furthermore, uranyl ions have played an important role in the processing of uranium ore, nuclear fuel and nuclear wastes [6]. It is worth mentioning that the hexavalent diuranyl ion, responsible for diverse structures of uranium, is the most important functional unit in the chemistry of uranium [6–10]. In addition, the divalent uranyl ion is highly stable and possesses two covalently bonded and linearly arranged terminal oxygen atoms that promote an equatorial arrangement for ligand coordination in its complexes [11]. The inertness of uranium-oxygen double bonds ($\text{U} = \text{O}$) is thought to be due to the unique confluence of electronic effects that lead to the formation of strong and unreactive $\text{U} = \text{O}$ bonds [1]. Furthermore, in the equatorial plane the uranyl ion can coordinate with four to six additional donor atoms lying perpendicular to

the axis of the uranium ion to form various geometric configurations [9,11–14]. Over the years, uranyl complexes have been the focus of growing interest in broad areas of research, including photochemistry, gas sorption, ion-exchange, catalysis, photocatalysis, proton conductivity and nuclear power, as well as in the extraction of uranium from the sea and its removal from the environment and the human body [10,15–20]. There are several reports of Schiff bases and their applications in the areas of catalysis, analytical chemistry (detecting and removing metal ions), fluorescence and quantitative analysis [21–23], biological activity and the evaluation of notable structural features [24]. Schiff base ligands, with multiple N and O donors, have always been a suitable choice for constructing versatile multinuclear architectures because of their rich coordination capacity, low cost and straightforward synthesis [25–29]. Here, we report a new and rare dinuclear uranyl(VI) coordination compound from a multisite Schiff base ligand, 1,3-bis(2-oxy-3-methoxybenzylidene)propan-2-olate [30]. This is the first report of the usage of 1,3-bis(2-oxy-3-methoxybenzylidene)propan-2-olate or its analogs in the preparation of a dinuclear uranyl(VI) coordination compound. Earlier reports of this ligand or its analogs reveal its usage in the synthesis of multinuclear complexes. The synthesized dinuclear uranyl(VI) coordination compound was investigated by various spectroscopic studies,

* Corresponding author.

E-mail address: mhashim@ksu.edu.sa (M. Azam).

single-crystal X-ray crystallography and DFT analyses. The sensing behavior and photoluminescence properties of the compound were also investigated. The studied coordination compound exhibited excellent fluorescence emission in water, making it a promising luminescent sensing material for detecting trace quantities of Pb (II) ions and the antibiotic cefuroxime. The results suggest the compound to be responsive to the Pb(II) ion and CFM (cefuroxime) with detection limits of 44.7 and 175 nM, respectively.

2. Experimental

2.1. Materials and methods

All the chemicals used in the experiments were procured from commercial sources. The ligand N,N'-bis(3-methoxysalicylidene)-1,3-diamino-2-propanol (H_3L) used in the complexation was prepared as reported [30]. C, H, N analyses were obtained by using an Elementar Vario EL analyzer. The Nuclear Magnetic Resonance (NMR) spectra were obtained using a JEOL-400 spectrometer in d_6 -DMSO. Fluorescence and FT-IR spectra were recorded on a RF-600 spectrofluorometer and a Perkin Elmer 621 spectrophotometer, respectively.

2.2. Preparation of the dinuclear uranyl coordination compound

Uranyl acetate (118 mg, 0.279 mmol.) was added to the yellow colored methanol solution of the ligand (50 mg, 1 mmol), resulting in the formation of red colored solution. A precipitate was obtained after continuous stirring for 5 h. The colored precipitate was isolated and dried in vacuum. The dried precipitate was dissolved in dichloromethane and yielded beautiful red crystals upon slow diffusion into *n*-pentane.

Color: Red. Molecular formula: $C_{22}H_{30}N_2O_{12}U_2$. Elemental analyses, Calculated: C, 26.68; H, 3.05; N, 2.83; Found: C, 26.68; H, 3.05; N, 2.83. IR (KBr, cm^{-1}): 1627, 1247, 1224, 2618, 738, 642, 916. ^1H NMR (δ , ppm, d_6 -DMSO): 8.38 (2H, $-\text{CH} = \text{N}$), 3.86 ($-\text{CH}_2$), 3.37 ($-\text{CH}$). ^{13}C NMR (δ , ppm, d_6 -DMSO): 167.5, 114.3–151.9, 70.4, 62.6, 56.03.

2.3. X-ray diffraction study

The X-ray crystallographic data for a red prism crystal of the synthesized coordination compound were obtained on a Rigaku Synergy Dualflex automatic diffractometer using mirror monochromated MoK α ($\lambda = 0.71073 \text{ \AA}$) radiation at 100.0(1) K with the ω scan mode. A summary of the crystallographic data and refinement details are summarized in Table 1. All calculations were made using SHELXS [31], SHELXL [32] and SHELXTL [33] programs. The parameters for electron atomic scattering factors were taken from the International Tables for Crystallography [34]. CCDC 1,963,636 contains the crystallographic data for the studied dinuclear uranyl coordination compound.

2.4. Computational details

With the aid of the Gaussian 09 program package [35], single point calculations using the CAM-B3LYP [36] and MPW1PW91 [37] methods combined with the 6-31G(d,p) basis sets for non-metal atoms and SARC-ZORA relativistic approach for uranium [38] were performed. Natural charges were calculated using the NBO program [39] and the Multiwfn [40] program was used to compute the atoms in molecules (AIM) topological parameters.

Table 1

Crystal and structure refinement data of the uranyl coordination compound.

Compound	Uranyl compound
Empirical formula	$C_{22}H_{30}N_2O_{12}U_2$
Formula weight	990.54
Crystal system, space group	triclinic, $P-1$ (No. 2)
Unit cell dimensions [\AA , $^\circ$]	$a = 10.1335(2)$ $b = 10.2215(2)$ $c = 13.6510(2)$ $\alpha = 84.3590(10)$ $\beta = 69.9070(10)$ $\gamma = 82.9010(10)$
Volume [\AA^3]	1315.36(4)
Z, Calculated density [Mg/m^3]	2, 2.501
$F(000)$	912
Crystal size [mm]	0.090, 0.083, 0.079
θ range for data collection [$^\circ$]	2.489 to 31.554
Index ranges	$-14 \leq h \leq 14$, $-15 \leq k \leq 14$, $-19 \leq l \leq 19$
Reflections collected / unique	85,011 / 8094 [$R_{\text{int}} = 0.0683$]
Completeness [%]	99.9% (to $\theta = 25.05^\circ$)
Data / restraints / parameters	8094 / 0 / 348
Goodness-of-fit on F^2	1.142
Final R indices [I greater than $2\sigma(I)$]	$R_1 = 0.0288$, $wR_2 = 0.0740$
R indices (all data)	$R_1 = 0.0330$, $wR_2 = 0.0752$
Largest diff. peak and hole [$e \text{ \AA}^{-3}$]	3.913, -2.606

2.5. Hirshfeld surface analysis

Topology analyses were performed using the Crystal Explorer 3.1 program [41] to determine the percentages of the different intermolecular interactions in the crystal structure of the studied coordination compound.

3. Results and discussion

The newly synthesized compound [Fig. 1] is an exceptional case of a dinuclear uranium coordination compound containing the pure or substituted 1,3-bis(2-oxy-3-methoxybenzylidene)propan-2-olate moiety (a propan-2-olate analog of salen). There are no other uranium compounds containing this ligand or its derivative. Among the coordination compounds of this ligand with other metals, tetrานuclear or higher multinuclear compounds are typically formed (such as bis(μ_3 -1,3-bis(3-oxysalicylideneamino)propan-2-olate)-bis(μ_2 -methoxy)-bis(dimethylformamide)-di-manganese(II)-di-manganese(III) dimethylformamide solvate [30] or bis(μ_4 -2,2'-(2-oxypropane-1,3-diyl)bis(nitrilomethylbenzylidene))bis(6-methoxyphenolato))-tetrakis(μ_3 -hydroxo)-bis(μ_2 -acetato-O,O')-bis(μ_2 -aqua)-bis(acetato-O)-bis(ethanol)-penta-copper-di-erbium dinitrate [42]). In the case of the few known dinuclear compounds, the ligand to metal ratio is mostly 1:1 (e.g., bis(μ_2 -1,3-bis(3-methoxysalicylideneamino)propan-2-olate)-di-iron(III) methanol solvate [30]), which is in opposition to the studied compound, for which this ratio is 1:2, or these compounds are heterometallic (for example catena-[$(\mu_3$ -2-ethoxy-6(((3-((3-ethoxy-2-(oxy)benzylidene)amino)-2-oxypropyl)imino)methyl)phenolato)-copper-sodium] [43]). The only compound with a similar composition, (μ_2 -acetato)-(m2-1,3-bis(2-oxy-3-methoxybenzylidene)propan-2-olate)-di-copper(II)dimethylformamide solvate [44], contains just two organic ligands in the inner coordination sphere (the studied compound contains four), and both are anionic; in the studied compound, two of the four ligands are neutral.

The studied compound possesses a complex molecule made of one triply deprotonated pentafunctional chelating-bridging (μ_2 -1,3-bis(2-oxy-3-methoxybenzylidene)propan-2-olate) ligand, two UO_2 cationic units, one difunctional bridging methanolate anion and two monofunctional methanol molecules. Each uranium

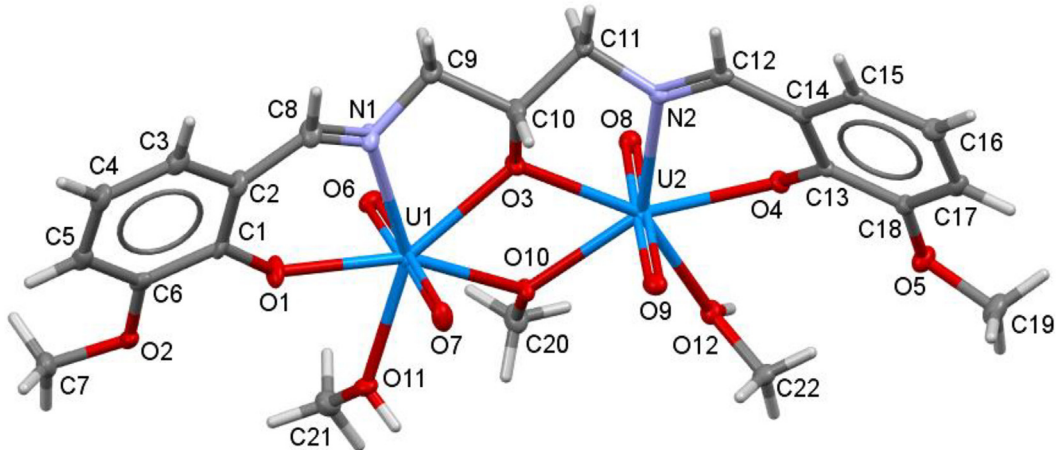


Fig. 1. The molecular structure of the studied dinuclear uranyl(VI) coordination compound, plotted with 50% probability of displacement ellipsoids for the non-hydrogen atoms. The hydrogen atoms are drawn as bars.

cation is seven-coordinated by one imine nitrogen atom, two alkoxide oxygen atoms of the chelating ligand, one alkoxide oxygen atom of a methanolate anion, one oxygen atom of methanol and two oxide ions. The coordination environments of the central atoms adopt a slightly pentagonal bipyramidal geometry [45] (Table 2) with oxide ions located at the polyhedral apexes. The uranium ions within the complex molecule are separated at 3.914(3) Å.

Table 2
Selected distances and angles of the uranyl coordination compound [Å, °].

Compound 1				
U1–O1	2.269(3)	U2–O3	2.394(3)	
U1–O3	2.339(3)	U2–O4	2.310(3)	
U1–O6	1.787(3)	U2–O8	1.785(3)	
U1–O7	1.781(3)	U2–O9	1.779(3)	
U1–O10	2.370(3)	U2–O10	2.363(3)	
U1–O11	2.451(3)	U2–O12	2.489(3)	
U1–N1	2.579(3)	U2–N2	2.533(3)	
U1–U2	3.91403(18)	N2–C12	1.286(5)	
N1–C8	1.294(5)	O4–C13	1.339(4)	
O1–C1	1.320(4)	O5–C18	1.371(4)	
O2–C6	1.384(5)	O3–C10	1.421(5)	
O7–U1–O6	177.39(13)	O9–U2–O8	178.78(12)	
O7–U1–O1	90.28(13)	O9–U2–O4	88.19(12)	
O6–U1–O1	89.19(13)	O8–U2–O4	90.63(11)	
O7–U1–O3	89.11(12)	O9–U2–O10	88.69(12)	
O6–U1–O3	93.03(12)	O8–U2–O10	92.27(12)	
O1–U1–O3	136.73(10)	O4–U2–O10	155.88(9)	
O7–U1–O10	92.06(12)	O9–U2–O3	91.10(12)	
O6–U1–O10	87.36(12)	O8–U2–O3	89.97(12)	
O1–U1–O10	155.41(10)	O4–U2–O3	136.93(9)	
O3–U1–O10	67.80(9)	O10–U2–O3	67.03(9)	
O7–U1–O11	87.47(12)	O9–U2–O12	89.13(11)	
O6–U1–O11	89.92(12)	O8–U2–O12	90.28(11)	
O1–U1–O11	77.38(10)	O4–U2–O12	75.20(9)	
O3–U1–O11	145.75(9)	O10–U2–O12	80.85(9)	
O10–U1–O11	78.28(9)	O3–U2–O12	147.87(9)	
O7–U1–N1	90.29(14)	O9–U2–N2	90.15(12)	
O6–U1–N1	91.94(13)	O8–U2–N2	89.74(12)	
O1–U1–N1	70.37(11)	O4–U2–N2	71.15(10)	
O3–U1–N1	66.37(10)	O10–U2–N2	132.77(9)	
O10–U1–N1	134.06(10)	O3–U2–N2	65.78(10)	
O11–U1–N1	147.66(10)	O12–U2–N2	146.35(9)	
O7–U1–U2	84.47(9)	O9–U2–U1	83.73(9)	
O6–U1–U2	96.43(10)	O8–U2–U1	97.49(9)	
O1–U1–U2	169.73(7)	O4–U2–U1	167.10(7)	
O3–U1–U2	34.67(7)	O10–U2–U1	34.26(6)	
O10–U1–U2	34.14(7)	O3–U2–U1	33.77(7)	
O11–U1–U2	111.11(6)	O12–U2–U1	114.59(6)	
N1–U1–U2	100.76(8)	N2–U2–U1	98.75(7)	

Å. All the atoms occupy general positions, but the coordination moiety possesses a pseudosymmetrical mirror plane going through the C10/O3/O10/C20 atoms. Therefore, pairs of analogous atoms of each molecule are related by a non-crystallographic pseudosymmetry element. Small differences in conformation of the terminal methoxybenzylidene moieties lead to a lack of pseudosymmetry within the crystal net. The coordination moiety is bent along the (μ_2 -1,3-bis(2-oxy-3-methoxybenzylidene)propan-2-olato) ligand, together with an inclination of the uranyl moieties. Analysis of the C–N bond lengths shows that the double bonds are fully localized within the benzylideneamino moieties (Table 2).

The crystal net of the studied compound contains both classical and non-classical hydrogen bonds (Table 3) as a result of the presence of medium strength and weak hydrogen bond donors [46]. The unitary graph set of the lowest degree consists of three ring motifs formed by O–H $\bullet\bullet\bullet$ O intramolecular hydrogen bonds: N₁R₂²(8) R₂²(8)R₂²(14). The binary graph set consists of multiple chain motifs [C₂²(15)C₄²(30)] composed from molecules assembled along the crystallographic [-1 1 1] axis into hydrogen bonded pillars. The π $\bullet\bullet\bullet$ π stacking interactions [47] expand these pillars into supramolecular layers propagating in the crystallographic [0 1 -1] plane. The weak C–H $\bullet\bullet\bullet$ O/π hydrogen bonds (Table 3) further expand the crystal net into the third dimension (Table 4).

3.1. Analysis of molecular packing

Hirshfeld surfaces mapped over d_{norm}, shape index, as well as the fingerprint plots of the most important interactions for the studied coordination compound are shown in Fig. 2. A summary of the most important contacts and their percentages are shown

Table 3
Hydrogen bonds geometry of the uranyl coordination compound [Å, °]. Cg(1) indicates the centroid of the six-membered phenyl ring containing the C1 atom.

D–H $\bullet\bullet\bullet$ A	d(D–H)	d(H $\bullet\bullet\bullet$ A)	d(D $\bullet\bullet\bullet$ A)	<(DHA)
O11–H11O $\bullet\bullet\bullet$ O1 ⁱ	0.82	2.52	3.046(4)	122.9
O11–H11O $\bullet\bullet\bullet$ O2 ⁱ	0.82	1.97	2.771(4)	166.8
O12–H12O $\bullet\bullet\bullet$ O4 ⁱⁱ	0.89	1.88	2.765(4)	169.4
C19–H19C $\bullet\bullet\bullet$ O8 ⁱⁱ	0.96	2.52	3.191(6)	127.4
C20–H20C $\bullet\bullet\bullet$ O12	0.96	2.58	3.214(5)	124.0
C20–H20C $\bullet\bullet\bullet$ O5 ⁱⁱ	0.96	2.50	3.370(6)	150.9
C21–H21A $\bullet\bullet\bullet$ O7 ⁱ	0.96	2.51	3.379(6)	150.8
C16–H16 $\bullet\bullet\bullet$ Cg(1) ⁱⁱⁱ	0.93	2.80	3.316(4)	115.8

Symmetry transformations used to generate equivalent atoms: (i) -x + 2, -y + 1, -z + 1; (ii) -x + 1, -y + 2, -z + 2; (iii) x-1, y, z + 1.

Table 4

Stacking interactions in the uranyl coordination compound [Å, °]. Cg(1) and Cg(2) indicate the centroids of the six-membered phenyl rings (R) containing the C1 and C13 atoms respectively, α is the dihedral angle between planes I and J, β is the angle between the Cg(I)-Cg(J) vector and the normal to plane I and d_p is the perpendicular distance of Cg(I) on the ring J plane.

R(I)…R(J)	Cg…Cg	α	β	d_p
Cg(1)…Cg(2) ⁱ	4.376(2)	41.65(19)	25.5	2.3154(17)
Cg(2)…Cg(1) ⁱⁱ	4.376(2)	41.65(19)	58.1	3.9482(16)
Cg(2)…Cg(1) ⁱⁱⁱ	5.389(2)	41.65(19)	41.0	1.3106(16)
Cg(2)…Cg(2) ^{iv}	3.819(2)	0.00(19)	32.9	3.2079(17)

Symmetry transformations used to generate rings: (i) $x + 1, y, z - 1$; (ii) $x - 1, y, z + 1$; (iii) $-x + 1, -y + 1, -z + 1$; (iv) $-x, -y + 2, -z + 2$.

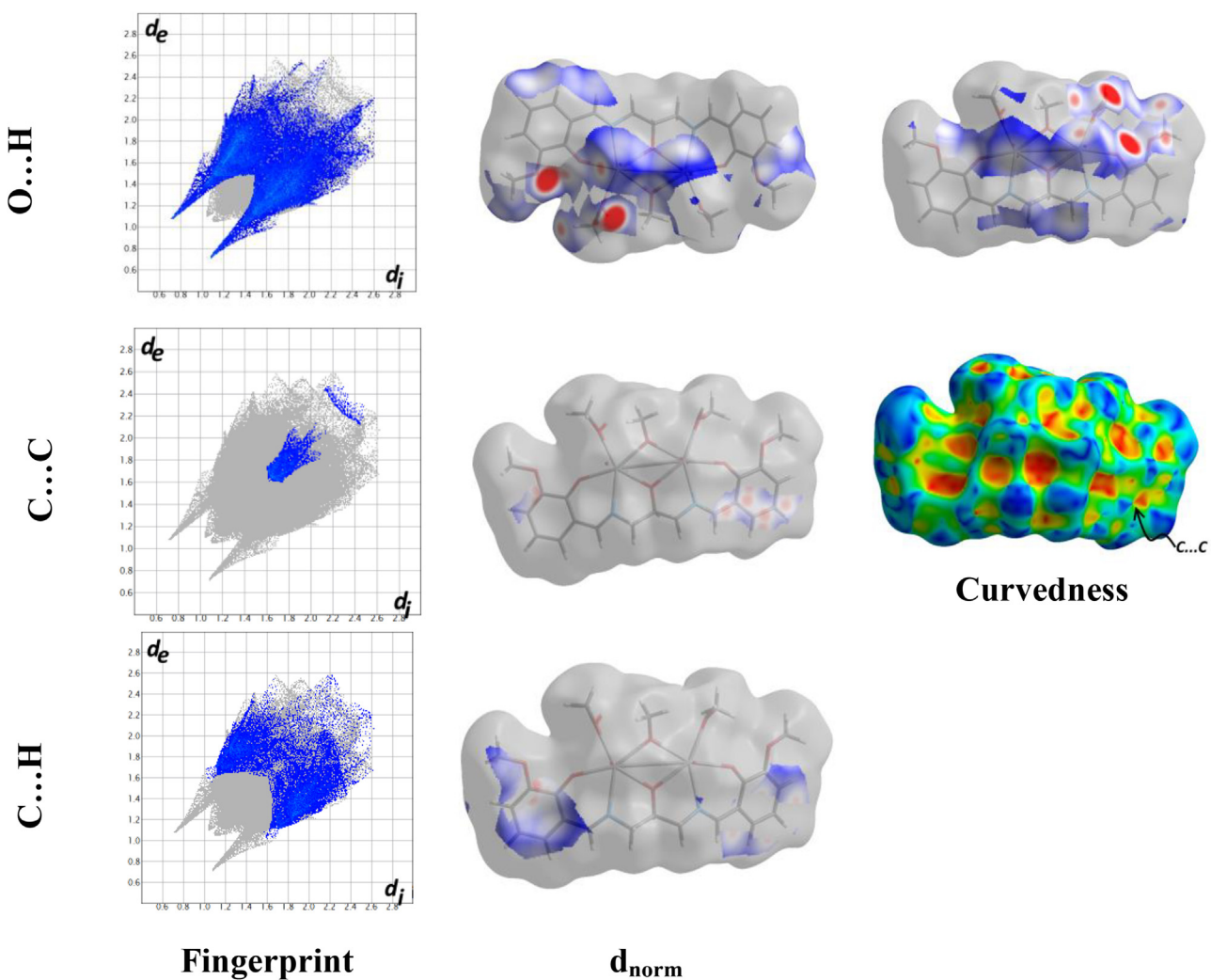


Fig. 2. The Hirshfeld surface analysis of the most important contacts in the studied dinuclear uranyl(VI) coordination compound.

in Fig. 3. In the studied system, H...H, O...H and C...H contacts are the most common intermolecular interactions in the molecular packing. The percentages of these contacts are 46.0, 33.9 and 14.8%, respectively. The H16...H22B (2.154 Å), O4...H12O (1.794 Å), O2...H11O (1.808 Å), C1...H17 (2.803 Å) and C2...H16 (2.813 Å) interactions display the shortest contacts. In addition, there are some π - π stacking interactions, as presented by a red-blue triangle in the shape index map, with C...C contacts of 3.1%. The shortest contact is 3.275 Å for the C14...C15 contact [Fig. 3].

3.2. DFT studies

3.2.1. AIM topological analysis

The studied dinuclear uranyl (VI) coordination compound showed that each of the uranium atoms has six U-O and one U-N bond. To investigate the nature and strength of these coordination interactions, we used atoms in molecules (AIM) calculations [48–56]. The results of the AIM topological parameters are collected in Table 5. The electron density ($\rho(r)$) values of the axial U = O

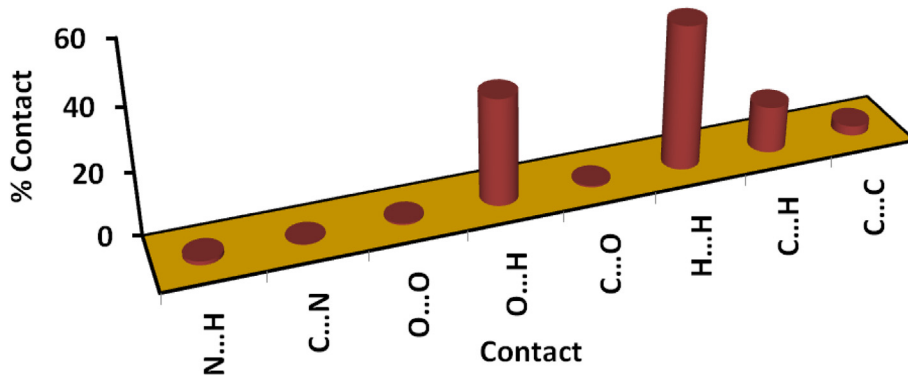


Fig. 3. Intermolecular interactions and their percentage in the studied compound.

bonds are significantly greater than 0.1 a.u., which is considered one of the main characteristics of covalent interactions. The total energy density ($H(r)$) values are significantly negative and the potential to kinetic energy density ($V(r)/G(r)$) ratios are significantly larger than unity. These observations reveal the high covalent characteristics of these bonds. On the contrary, the U-O and U-N interactions have $p(r) < 0.1$ a.u. These interactions have very small $H(r)$ values close to zero, whereas the $V(r)/G(r)$ ratios are close to unity. These results indicate that the equatorial U-O and U-N interactions mainly belong to closed shell interactions, which likely have low covalent character. Fig. 4 shows excellent straight-line correlations between the U-O distances and $p(r)$, as well as the calculated interaction energies [55].

3.2.2. Natural population analysis

The interactions between the uranium ion and donor atoms were analyzed via the NBO method. The NBO interaction energies

($E^{(2)}$) for the different U-O and U-N bonds are collected in Table 6. It is clear that the organic ligand donor atoms, as well as the O-sites of the methanol and methoxide ligand groups, coordinate to the U2 site more strongly than the coordination with the U1 site. The net interaction energies are calculated to be 583.5 and 694.9 kcal/mol for U1 and U2, respectively. The U-O interactions with the organic ligand are the strongest among all the U-O interactions, for which the U-O bonds with the bridged methoxide ion (33.87–107.17 kcal/mol) and terminal methanol molecules (90.83–100.54 kcal/mol) are the weakest.

The IR spectrum revealed a strong characteristic peak at 1627 cm^{-1} , attributed to the imine functional group [27,57]. Medium-intensity bands due to $\nu_{(\text{U}-\text{O})}$ bonds appeared at 738 cm^{-1} and the band exhibited at 642 cm^{-1} is attributed to the U-N linkage [27]. The strong band at 916 cm^{-1} is assigned to the characteristic

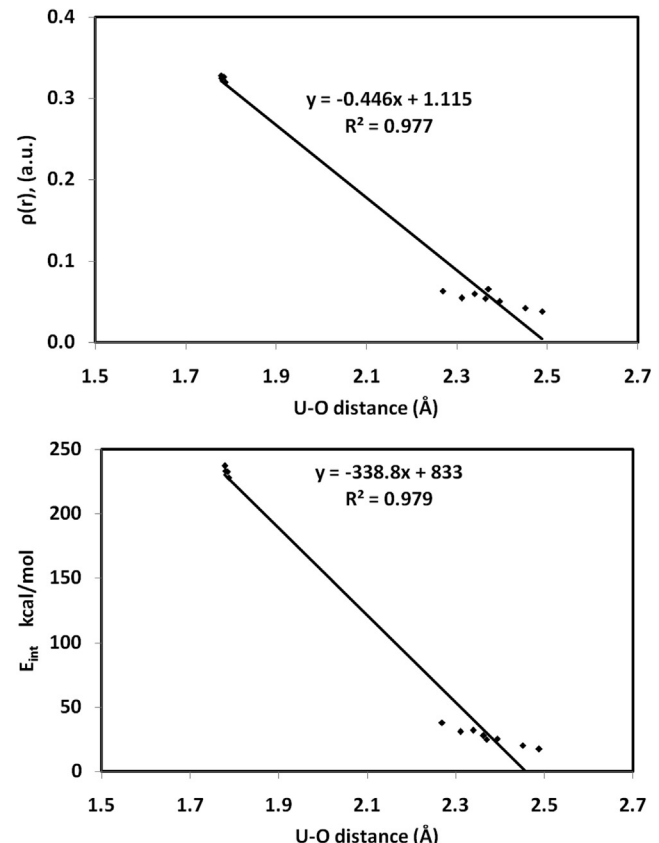
Fig. 4. Correlations between the U-O distances with $\rho(r)$ and interaction energies using the Espinosa relation.^a kcal/mol.

Table 5
AIM topological parameters (a.u.) of the U-N, and U-O interactions.

Bond	$\rho(r)$	$G(r)$	$V(r)$	$H(r)$	$V(r)/G(r)$	E_{int}^{a}
mPW1PW91						
U1-O1	0.0632	0.1229	-0.1211	0.0018	0.985	38.00
U1-O6	0.3196	0.4205	-0.7266	-0.3061	1.728	227.97
U1-O10	0.0655	0.0788	-0.0794	-0.0007	1.009	24.92
U1-O3	0.0599	0.1004	-0.1016	-0.0012	1.012	31.87
U1-O11	0.0426	0.0683	-0.0641	0.0042	0.939	20.12
U1-O7	0.3247	0.4286	-0.7436	-0.3151	1.735	233.32
U1-N1	0.0345	0.0553	-0.0514	0.0039	0.929	16.12
U2-O3	0.0506	0.0830	-0.0808	0.0022	0.974	25.36
U2-O10	0.0539	0.0905	-0.0885	0.0020	0.978	27.78
U2-O4	0.0544	0.1014	-0.0985	0.0029	0.972	30.92
U2-N2	0.0401	0.0633	-0.0607	0.0025	0.960	19.06
U2-O9	0.3285	0.4332	-0.7560	-0.3228	1.745	237.20
U2-O8	0.3267	0.4239	-0.7418	-0.3180	1.750	232.75
U2-O12	0.0380	0.0601	-0.0554	0.0048	0.921	17.37
CAM-B3LYP						
U1-O1	0.0836	0.0930	-0.1005	-0.0075	1.081	31.53
U1-O6	0.3221	0.4186	-0.7278	-0.3092	1.739	228.35
U1-O10	0.0528	0.0889	-0.0864	0.0025	0.972	27.11
U1-O3	0.0573	0.0982	-0.0969	0.0013	0.987	30.39
U1-O11	0.0419	0.0680	-0.0632	0.0048	0.929	19.83
U1-O7	0.3242	0.4311	-0.7449	-0.3139	1.728	233.72
U1-N1	0.0358	0.0563	-0.0530	0.0033	0.941	16.63
U2-O3	0.0524	0.0848	-0.0836	0.0012	0.985	26.22
U2-O10	0.0647	0.0817	-0.0812	0.0005	0.994	25.48
U2-O4	0.0774	0.0833	-0.0884	-0.0051	1.062	27.75
U2-N2	0.0409	0.0641	-0.0616	0.0025	0.962	19.33
U2-O9	0.3256	0.4323	-0.7494	-0.3171	1.733	235.12
U2-O8	0.3252	0.4211	-0.7357	-0.3146	1.747	230.84
U2-O12	0.0405	0.0622	-0.0581	0.0040	0.935	18.24

Table 6

The interaction energies ($E^{(2)}$) calculated using the NBO method for the U-N and U-O interactions using the mPW1PW91 method.

Bond	$E^{(2)}$
U1-N1	93.21
U1-O1	201.23
U1-O3	164.38
U1-O10	33.87
U1-O11	90.83
U2-N2	111.83
U2-O3	178.94
U2-O4	196.38
U2-O10	107.17
U2-O12	100.54

linear uranyl ion [Supplementary Information Fig. S1] [58]. The ^1H NMR spectrum displayed the characteristic signal due to the azomethine proton at δ 8.38 ppm. Multiplets due to the aromatic proton were observed at δ 6.78–7.24 ppm. The –CH and –CH₂ protons were observed at δ 3.37 and 3.86 ppm, respectively [Supplementary Information Fig. S2]. The ^1H NMR spectral findings were further confirmed by ^{13}C NMR data, which clearly suggested the presence of an azomethine carbon atom at δ 167.5 ppm [Supplementary Information Fig. S3].

3.2.3. Photoluminescence behavior

The fluorescence spectra, monitored at 500–650 nm with an emission wavelength at 300 nm, showed two excitation peaks at 273 and 302 nm. On comparing the emission spectra at both exci-

tation peaks, the emission spectrum at 302 nm showed greater fluorescence intensity and a bathochromic shift at 603 nm due to a lower-lying non-emissive LMCT arising from ligand-U(VI) interactions [Fig. 5] [59]. The emission spectrum of the studied compound exhibited a number of vibronic bands, showing electron transfer from the ligand to the 5f shell of uranyl ion in the emitting state [60,61]. Thus, it can be assumed that the excited molecules display radical-like activity in the excited state [62,63].

To assess the selective sensing behavior of the studied dinuclear uranyl(VI) coordination compound, quantitative fluorescence titration experiments were used to investigate the sensing behaviors for Fe^{3+} , Co^{2+} , Ni^{2+} , Cu^{2+} , Zn^{2+} , Pb^{2+} , Sb^{3+} and Ln^{3+} ions in aqueous medium. Fig. 6 reveals that the fluorescence property of the studied coordination compound is almost independent of the concentration (150 to 900 nM) of the metal ions, but it remains dependent on Pb^{2+} ions. Although the Fe^{3+} ion showed fairly good fluorescence quenching behavior, it was found to be less sensitive as compared to Pb^{2+} ions. The sensing behavior for Pb^{2+} ions with the uranyl compound can be explained by electron transfer phenomenon between the metal ions and the uranyl compound. The Pb^{2+} ion possesses a large number of low energy empty or partially filled d-orbitals, which may lead to easy electron transfer between the uranyl coordination compound and the Pb^{2+} ions [61].

Fig. 6 clearly shows that the fluorescence emission intensity decreases monotonically upon increasing the concentration of Pb^{2+} ions from 0.5 to 3 mL (150 to 900 nM). Thus, the obtained results confirm that the studied compound is highly sensitive and selective sensing for Pb^{2+} ions in an aqueous suspension. The fluorescence quenching efficiency can be quantitatively studied by the Stern-Volmer equation:

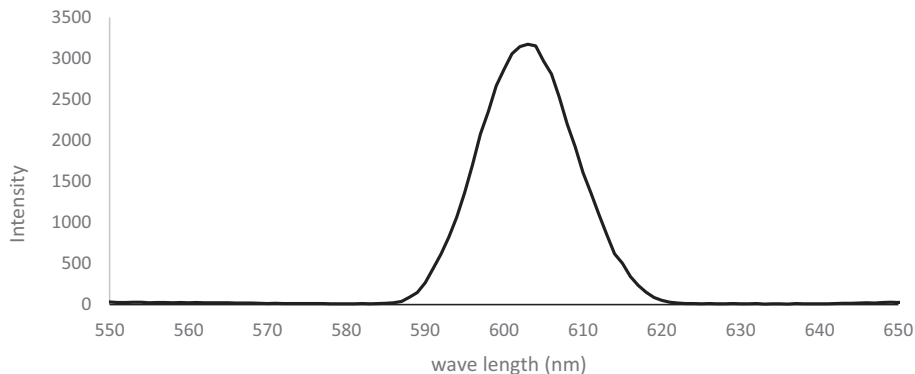


Fig. 5. Photoluminescence emission spectrum of the dinuclear uranyl(VI) coordination compound on excitation at 302 nm.

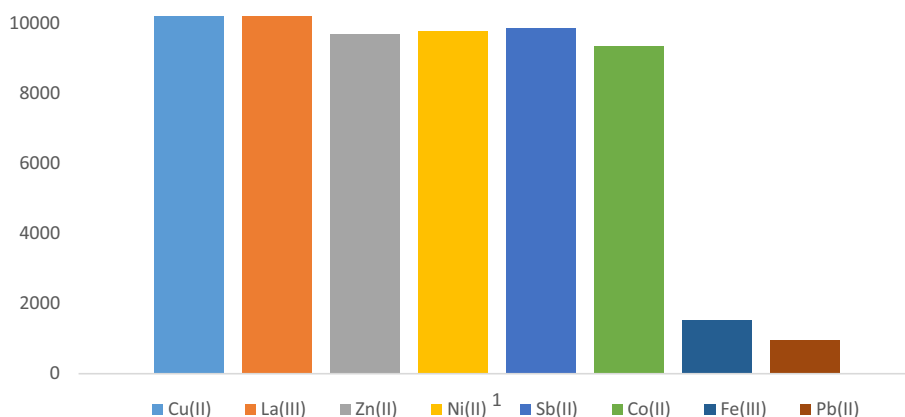


Fig. 6. Fluorescence quenching of the dinuclear uranyl(VI) coordination compound by different metal ions at room temperature.

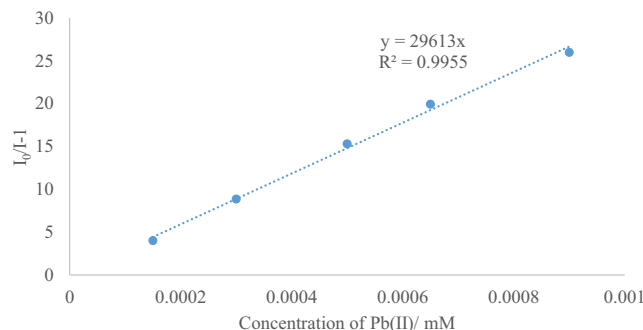


Fig. 7. Stern–Volmer plot for $\text{Pb}(\text{II})$ ions.

$$(I_0/I)/[M] = 1 + K_{\text{SV}}[M] \quad (1)$$

where K_{SV} is the quenching constant (mM^{-1}), $[M]$ is the molar concentration of the analyte, and I_0 and I are the luminescence intensities before and after addition of the analyte, respectively. Detailed K_{SV} analysis further revealed a good linear correlation ($R = 0.9955$) between the quenching efficiency and the amount of Pb^{2+} ions used at low concentrations (150 to 900 nM), as indicated in Fig. 7.

Fig. 7 reveals that I_0/I in the Stern–Volmer equation linearly increased upon increasing the concentration of Pb^{2+} ions. Therefore, it can be concluded that the quenching mechanism is static and the quenching by the Pb^{2+} ion is due to the formation of a non-fluorescent complex between the excited fluorophore, which is the studied compound, and the $\text{Pb}(\text{II})$ ions [61].

On the basis of the experimental results mentioned in Fig. 7, the K_{SV} values were calculated to be $2.96 \times 10^4 \text{ mM}^{-1}$ for the studied dinuclear uranyl coordination compound. In addition, based on the K_{SV} values and the standard error (σ) for three repetitive fluorescence experiments of blank solutions, the detection limit ($3\sigma/K_{\text{SV}}$) was also calculated and found to be 44.7 nM (9.3 ppb), indicating the high selective sensitivity of the studied compound towards Pb^{2+} ions. Thus, the studied compound can be considered a potential candidate for the selective sensing of Pb^{2+} ions.

Furthermore, the excellent luminescence behavior of the studied compound prompted us to apply it as a potential fluorescent sensor for detecting trace quantities of antibiotics, such as CFM (Cefuroxime), FLZ (Fluconazole) and AXL (Amoxicillin). To explore the ability of the studied compound to sense trace quantities of antibiotics, fluorescence-quenching titrations were performed by

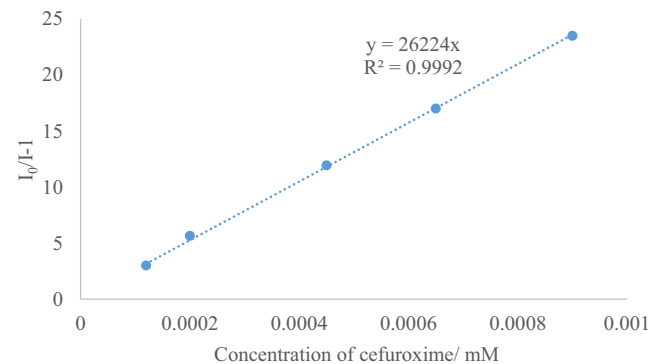


Fig. 9. Stern–Volmer plot of cefuroxime.

gradually adding antibiotics to an aqueous suspension of the studied compound. Fig. 8 reveals the dramatic quenching in the emission intensity of the studied compound upon incremental addition of CFM, which might be attributed to a charge effect and energy transfer between the studied compound and CFM. It is obvious that the highest fluorescence quenching was noticed for CFM. The fluorescence quenching efficiency for the antibiotics was of the order: CFM > AXL > FLZ.

The fluorescent quenching efficiency can be quantitatively explained by the Stern – Volmer relationship (SV), as described in equation (1). The SV plot for CFM is nearly linear at low concentrations, 120 to 900 nM (Fig. 9). The studied compound has the highest K_{SV} value of $2.62 \times 10^4 \text{ mM}^{-1}$. On the basis of the K_{SV} values and the standard error (σ) for three repetitive fluorescence experiments of blank solutions, the detection limit ($3\sigma/K_{\text{SV}}$) towards CFM was calculated to be 74.2 ppb (or 175 nM), revealing the studied compound to have a high quenching efficiency towards CFM (Fig. 9), thus suggesting it could be a reliable sensing material for detecting CFM in aqueous solution.

4. Conclusion

In summary, we have successfully designed a new dinuclear uranyl(VI) coordination compound using a multisite salen ligand. The titled compound exhibited a high quenching response and excellent selectivity for Pb^{2+} ions and cefuroxime, making it a potential candidate for sensing purposes in aqueous solution.

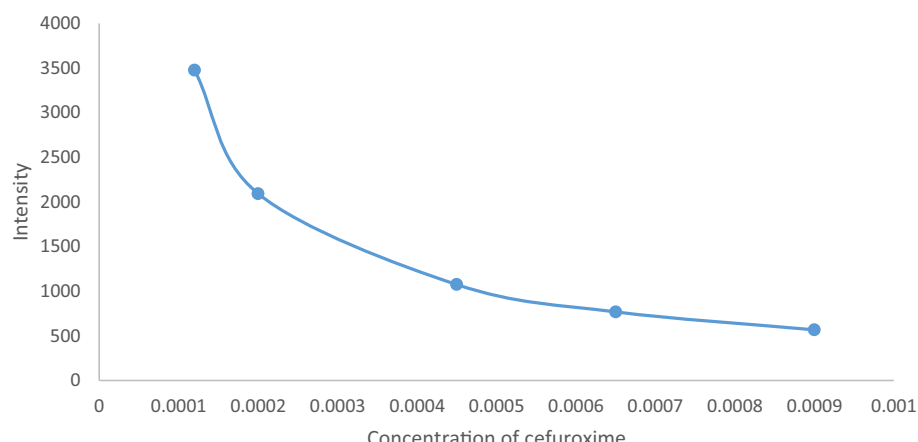


Fig. 8. Fluorescence quenching spectrum of the dinuclear uranyl(VI) coordination compound at various concentrations of cefuroxime.

Declaration of Competing Interest

The authors declare that they have no known competing financial interests or personal relationships that could have appeared to influence the work reported in this paper.

Acknowledgements

The authors would like to extend their sincere appreciation to the Deanship of Scientific Research at King Saud University for funding this work through research group project number RG -1436-003. R.K. and A.T.K. acknowledge the financial assistance allocated by the Ministry of Science and Higher Education to the Institute of General and Ecological Chemistry, Lodz University of Technology.

Appendix A. Supplementary data

Supplementary data to this article can be found online at <https://doi.org/10.1016/j.poly.2020.114745>.

References

- [1] N. Greenwood, A. Earnshaw, *Chemistry of the Elements*, Second edition., Butterworth-Heinemann, Burlington, MA, 2010.
- [2] T.W. Hayton, J.M. Boncella, B.L. Scott, P.D. Palmer, E.R. Batista, P.J. Hay, Synthesis of imido analogs of the uranyl ion, *Science* 310 (2005) 1941–1943.
- [3] R.J. Baker, The coordination and organometallic chemistry of UI3 and U(N(SiMe₃)₂)₃: Synthetic reagents par excellence, *Coord. Chem. Rev.* 256 (23–24) (2012) 2843–2871.
- [4] D.L. Clark, D.E. Hobart, M.P. Neu, Actinide Carbonte Complexes and Their Importance in Actinide Environmental Chemistry, *Chem. Rev.* 95 (1) (1995) 25–48.
- [5] J.J. Katz, G.T. Seaborg and L.R. Morss, The Chemistry of the Actinide Elements, vol. 1, second ed., Chapman and Hall, New York, 1986.
- [6] J.J. Katz, G. T. Seaborg and L.R. Morss, The Chemistry of the Actinide Elements (Chapman and Hall, New York, ed. 2, 1986).
- [7] A.E. Comyns, The coördination chemistry of the actinides, *Chem. Rev.* 60 (2) (1960) 115–146.
- [8] R.N. Sylva, M.R. Davidson, The hydrolysis of metal ions. Part 2. Dioxouranium (VI), *J. Chem. Soc., Dalton Trans.* (3) (1979) 465, <https://doi.org/10.1039/dt9790000465>.
- [9] J.L. Bjorklund, M.M. Pyrch, M.C. Basile, S.E. Mason, T.Z. Forbes, Actinyl-cation interactions: experimental and theoretical assessment of [Np(VI)O₂Cl₄]²⁻ and [U(VI)O₂Cl₄]²⁻ systems, *Dalton Trans.* 48 (2019) 8861–8871.
- [10] M.B. Andrews, C.L. Cahill, In situ oxalate formation during hydrothermal synthesis of uranyl hybrid materials, *CrystEngComm* 13 (23) (2011) 7068, <https://doi.org/10.1039/c1ce05934c>.
- [11] N. Zhang, Yong-Heng Xing, Feng-Ying Bai, A uranyl-organic framework featuring two-dimensional graphene-like layered topology for efficient iodine and dyes capture, *Inorg. Chem.* 58 (58) (2019) 6866–6876.
- [12] R.G. Denning, *Struct. Bonding (Berlin)* 79 (1992) 215–276.
- [13] M.B. Jones, A.J. Gaunt, Recent developments in synthesis and structural chemistry of nonaqueous actinide complexes, *Chem. Rev.* 113 (2) (2013) 1137–1198.
- [14] G.E. Gomez, J.A. Ridenour, N.M. Byrne, A.P. Shevchenko, C.L. Cahill, Novel heterometallic uranyl-transition metal materials: structure, topology, and solid state photoluminescence properties, *Inorg. Chem.* 58 (2019) 7243–7254.
- [15] J. Sessler, P. Melfi, G. Pantos, Uranium complexes of multidentate N-donor ligands, *Coord. Chem. Rev.* 250 (7–8) (2006) 816–843.
- [16] A.U. Czaja, N. Trukhan, U. Müller, Industrial applications of metal-organic frameworks, *Chem. Soc. Rev.* 38 (5) (2009) 1284, <https://doi.org/10.1039/b804680h>.
- [17] P.O. Adelani, T.E. Albrecht-Schmitt, Differential ion exchange in elliptical uranyl diphosphonate nanotubes, *Angew. Chem. Int. Ed.* 49 (47) (2010) 8909–8911.
- [18] W. Yang, S. Dang, H. Wang, T. Tian, Q.-J. Pan, Z.-M. Sun, Synthesis, structures, and properties of uranyl hybrids constructed by a variety of mono- and polycarboxylic acids, *Inorg. Chem.* 52 (21) (2013) 12394–12402.
- [19] W. Xu, Zhen-Xiu Si, M. Xie, Lin-Xia Zhou, Yue-Qing Zheng, Bridging Ligands: Crystal Structures, Luminescence and Photocatalytic Degradation of Tetracycline Hydrochloride, *Cryst. Growth Des.* 17 (2017) 2147–2157.
- [20] S. Hadjithoma, M.G. Papanikolaou, E. Leontidis, T.A. Kabanos, A.D. Keramidas, Bis(hydroxylamino)triazines: High Selectivity and Hydrolytic Stability of Hydroxylamine-Based Ligands for Uranyl Compared to Vanadium(V) and Iron(III), *Inorg. Chem.* 57 (2018) 7631–7643.
- [21] B.K. Kundu, V. Chhabra, N. Malviya, R. Ganguly, G.S. Mishra, S. Mukhopadhyay, Mechanistic and thermodynamical aspects of pyrene based fluorescent probe to detect picric acid, *Micropor. Mat.* 271 (2018) 100–117.
- [22] Yikang Yan, Gutha Yuvaraja, Chunjiang Liu, Lingjun Kong, Kai Guo, Guda Mallikarjuna Reddy, Grigory V. Zyryanov, Removal of Pb(II) ions from aqueous media using epichlorohydrin crosslinked chitosan Schiff's base@Fe₃O₄ (ECCSB@Fe₃O₄), *Int. J. Biol. Macromol.* 117 (2018) 1305–1313.
- [23] Somaye Shahraki, Hojjat Samareh Delarami, Magnetic chitosan-(d-glucosimine methyl)benzaldehyde Schiff base for Pb²⁺ ion removal. Experimental and theoretical methods, *Carbohydr. Polym.* 200 (2018) 211–220.
- [24] Barbara Miroslaw, Beata Cristovão, Zbigniew Hnatejko, Halogen bonded lamellar motifs in crystals of Schiff base ZnII-LnIII-ZnII coordination compounds – Synthesis, structure, Hirshfeld surface analysis and physicochemical properties, *Polyhedron* 166 (2019) 83–90.
- [25] Lin Jiang, Dong-Yan Zhang, Jing-Jing Suo, Wen Gu, Jin-Lei Tian, Xin Liu, Shi-Ping Yan, Synthesis, magnetism and spectral studies of six defective dicubane tetranuclear {M 4 O 6} (M = Ni II, Co II, Zn II) and three trinuclear Cd II complexes with polydentate Schiff base ligands, *Dalton Trans.* 45 (25) (2016) 10233–10248.
- [26] M. Azam, S.I. Al-Resayes, Phenoxy-bridged binuclear Zn(II) complex holding salen ligand: Synthesis and Structural Characterization, *J. Molecular Struct.* 1107 (2016) 77–81.
- [27] M. Azam, S.I. Al-Resayes, G. Velmurugan, P. Venuvanalingam, Jörg Wagler, E. Kroke, Novel Uranyl(VI) Complex incorporating propylene-bridged salen-type N2O2-Ligand: A Structural and Computational Approach, *Dalton Trans.* 44 (2015) 568–577.
- [28] Stavroula I. Sampani, Edward Loukopoulos, Mohammad Azam, Kieran Griffiths, Alaa Abdul-Sada, Graham Tizzard, Simon Coles, Albert Escuer, Athanassios Tsipis, George E. Kostakis, Polynuclear ampyrone based 3d coordination clusters, *CrystEngComm* 20 (10) (2018) 1411–1421.
- [29] Mohammad Azam, Saud I. Al-Resayes, Agata Trzesowska-Kruszynska, Rafal Kruszynski, Pawan Kumar, Suman L. Jain, Seven-coordinated chiral uranyl(VI) salen complex as effective catalyst for C–H bond activation of dialkylanilines under visible light, *Polyhedron* 124 (2017) 177–183.
- [30] Y. Lan, G. Novitchi, R. Clerac, J. Tang, N.T. Madhu, I.J. Hewitt, C.E. Anson, S. Brooker, A.K. Powell, Di-, tetra- and hexanuclear iron(III), manganese(II/III) and copper(II) complexes of Schiff-base ligands derived from 6-substituted-2-formylphenols, *Dalton Trans.* (2009) 1721–1727.
- [31] G.M. Sheldrick, SHELXT – Integrated space-group and crystal-structure determination, *Acta Cryst. A71* (2015) 3–8.
- [32] G. M. Sheldrick, Crystal structure refinement with SHELXL, *Acta Cryst. C71* (2015) 3–8.
- [33] G.M. Sheldrick, A short history of SHELX, *Acta Crystallogr. A Found. Crystallogr.* 64 (1) (2008) 112–122.
- [34] E. Prince (ed.) International Tables for Crystallography, Volume C: Mathematical, physical and chemical tables, 3rd Edition, Kluwer Academic Publishers, Dordrecht, 2004.
- [35] a) M.J. Frisch, G.W. Trucks, H.B. Schlegel, G.E. Scuseria, M.A. Robb, J.R. Cheeseman, G.Scalmani, V.Barone, B.Mennucci, G.A. Petersson, H.Nakatsuji, M. Caricato, X. Li, H.P. Hratchian, A.F. Izmaylov, J. Bloino, G.Zheng, J.L. Sonnenberg, M. Hada, M. Ehara, K. Toyota, R. Fukuda, J. Hasegawa, M. Ishida, T. Nakajima, Y. Honda, O. Kitao, H. Nakai, T. Vreven, J.A. Montgomery, Jr., J.E. Peralta, F. Ogliaro, M. Bearpark, J.J. Heyd, E. Brothers, K.N. Kudin, V.N. Staroverov, R. Kobayashi, J. Normand, K. Raghavachari, A. Reed, J.C. Burant, S.S. Iyengar, J. Tomasi, M. Cossi, N. Rega, J.M. Millam, M. Klene, J.E. Knox, J.B. Cross, V. Bakken, C. Adamo, J. Jaramillo, R. Gomperts, R.E. Stratmann, O. Yazyev, A.J. Austin, R. Cammi, C. Pomelli, J.W. Ochterski, R.L. Martin, K. Morokuma, V.G. Zakrzewski, G.A. Voth, P. Salvador, J.J. Dannenberg, S. Dapprich, A.D. Daniels, O. Farkas, J.B. Foresman, J.V. Ortiz, J. Cioslowski, D.J. Fox, *GAUSSIAN 09*. Revision A02. Gaussian Inc., Wallingford CT, USA (2009), and b) GaussView, Version 4.1, R. Dennington II, T. Keith, J. Millam, Semichem Inc., Shawnee Mission, KS, (2007).
- [36] X. Xu, W.A. Goddard III, The X3LYP extended density functional for accurate descriptions of nonbond interactions, spin states, and thermochemical properties, *Proc. Natl. Acad. Sci. USA* 101 (2004) 2673–2677.
- [37] C. Adamo, V. Barone, Exchange functionals with improved long-range behavior and adiabatic connection methods without adjustable parameters: the mPW and mPW1PW models, *J. Chem. Phys.* 108 (1998) 664–675.
- [38] a) D. Feller, The Role of Databases in Support of Computational Chemistry Calculations *J. Comp. Chem.* 17 (1996) 1571–1586; b) K.L. Schuchardt, B.T. Didier, T. Elsethagen, L. Sun, V. Gurumoorthy, J. Chase, J. Li, T. L. Windus, Basis Set Exchange: A Community Database for Computational Sciences, *J. Chem. Inf. Model.* 47 (2007) 1045–1052; c) D.A. Pantazis, F. Neese, All-Electron Scalar Relativistic Basis Sets for the Actinides, *J. Chem. Theory Comput.*, 7 (2011) 677–684.
- [39] E.D. Glendening, A.E. Reed, J.E. Carpenter, F. Weinhold, NBO Version 3.1, CI, University of Wisconsin, Madison, 1998.
- [40] T. Lu, F. Chen, Multifwfn: a multifunctional wavefunction analyzer, *J. Comp. Chem.* 33 (2012) 580–592.
- [41] M.J. Turner, J.J. McKinnon, S.K. Wolff, D.J. Grimwood, P.R. Spackman, D. Jayatilaka, M.A. Spackman, Crystal Explorer 17, 2017, University of Western Australia, <http://hirshfeldsurface.net>.
- [42] V. Chandrasekhar, A. Dey, S. Das, M. Rouxieres, R. Clerac, Syntheses, Structures, and Magnetic Properties of a Family of Heterometallic Heptanuclear [Cu₅Ln₂] (Ln = Y(III), Lu(III), Dy(III), Ho(III), Er(III), and Yb(III)) Complexes: Observation of SMM behavior for the Dy(III) and Ho(III) Analogues, *Inorg. Chem.* 52 (2013) 2588–2598.
- [43] Debabrata Biswas, Partha Pratim Chakrabarty, Sandip Saha, Atish Dipankar Jana, Dieter Schollmeyer, Santiago García-Granda, Ligand mediated structural

- diversity and role of different weak interactions in molecular self-assembly of a series of copper(II)-sodium(I) Schiff-base heterometallic complexes, *Inorg. Chim. Acta* 408 (2013) 172–180.
- [44] A. Elmali, C.T. Zeyrek, Y. Elerman, Crystal structure, magnetic properties and molecular orbital calculations of a binuclear copper(II) complex bridged by an alkoxo-oxygen atom and an acetate ion, *J. Mol. Struct.* 693 (1–3) (2004) 225–234.
- [45] D.L. Kepert, Aspects of the Stereochemistry of Seven-Coordination, in *Progress in Inorganic Chemistry*, Volume 25 pp 41–144 (ed S. J. Lippard), John Wiley & Sons, Inc., Hoboken, NJ, USA (1979).
- [46] G.R. Desiraju, T. Steiner, *The Weak Hydrogen Bond in Structural Chemistry and Biology*, Oxford University Press, Oxford, 1999.
- [47] Rafal Kruszynski, Tomasz Sierański, Can Stacking Interactions Exist Beyond the Commonly Accepted Limits?, *Cryst Growth Des.* 16 (2) (2016) 587–595.
- [48] R.F.W. Bader, *Atoms in molecules: a quantum theory*, Oxford University Press, Oxford, U.K., 1990.
- [49] C.F. Matta, J. Hernandez-Trujillo, T.-H. Tang, T.-H.; R.F.W. Bader, Hydrogen-hydrogen bonding: a stabilizing interaction in molecules and crystals, *Chem. Eur. J.* 9 (2003) 1940–1951.
- [50] S.J. Grabowski, A. Pfitzner, M. Zabel, A.T. Dubis, M. Palusiak, Intramolecular H...H Interactions for the Crystal Structures of [4-(*(E*)-But-1-enyl)-2,6-dimethoxyphenyl]pyridine-3-carboxylate and [4-(*(E*)-Pent-1-enyl)-2,6-dimethoxyphenyl]pyridine-3-carboxylate; DFT Calculations on Modeled Styrene Derivatives, *J. Phys. Chem. B* 108 (2004) 1831–1837.
- [51] C.F. Matta, N. Castillo, R.J. Boyd, Characterization of a closed-shell fluorine-fluorine bonding interaction in aromatic compounds on the basis of the electron density, *J. Phys. Chem. A* 109 (2005) 3669–3681.
- [52] A. Martín Pendás, Evelio Francisco, Miguel A. Blanco, Carlo Gatti, Bond Paths as Privileged Exchange Channels, *Chem. Eur. J.* 13 (33) (2007) 9362–9371.
- [53] M.F. Bobrov, G.V. Popova, V.G. Tsirelson, A topological analysis of electron density and chemical bonding in cyclophosphazenes $P_nN_nX_{2n}$ ($X = H, F, Cl$; $n = 2, 3, 4$), *Russ. J. Phys. Chem.* 80 (2006) 584–590.
- [54] (a) C. Gatti Chemical bonding in crystals: new directions, *Z. Kristallogr.* 220 (2005) 399–457. (b) G.V. Gibbs, R.T. Downs, D.F. Cox, N.L. Ross, Jr. M.B. Boisen, K.M. Rosso, Characterization of a Closed-Shell Fluorine–Fluorine Bonding Interaction in Aromatic Compounds on the Basis of the Electron Density, *J. Phys. Chem. A* 112 (2008) 3693–3699.
- [55] E. Espinosa, E. Molins, C. Leconte, Hydrogen bond strengths revealed by topological analyses of experimentally observed electron densities, *Chem. Phys. Lett.* 285 (1998) 170–173.
- [56] D. Cremer, E. Kraka, Chemical Bonds without Bonding Electron Density – Does the Difference Electron-Density Analysis Suffice for a Description of the Chemical Bond?†, *Angew. Chem., Int. Ed. Engl.* 23 (1984) 627–628.
- [57] K. Nakamoto, *Infrared and Raman Spectra of Inorganic and Coordination Compounds, Part B: Applications in Coordination, Organometallic and Bioinorganic Chemistry*, sixth ed., John Wiley & Sons Inc, New York, New Jersey, 2009.
- [58] R. Kannappan, S. Tanase, D.M. Tooke, A.L. Spek, I. Mutikainen, U. Turpeinen, J. Reedijk, Separation of actinides and lanthanides: crystal and molecular structures of N, N' -bis(3,5-di-t-butylsalicylidene)-4,5-dimethyl-1,2-phenylenediamine and its uranium complex, *Polyhedron* 23 (2004) 2285–2291.
- [59] H.C. Hardwick, D.S. Royal, M. Hellwell, S.J.A. Pope, L. Ashton, R. Goodacre, C.A. Sharrad, Structural, spectroscopic and redox properties of uranyl complexes with a maleonitrile containing ligand†, *Dalton Trans.* 40 (2011) 5939–5952.
- [60] C.P. Baird, T.J. Kemp, Luminescence, spectroscopy, lifetimes and quenching mechanisms of excited states of uranyl and other actinide ions, *Prog. React. Kin.* 22 (1997) 87–139.
- [61] Z. Libus', Absorption spectra of uranium(VI) complexes in solutions, *J. Inorg. Nucl. Chem.* 24 (1962) 619–631.
- [62] H.D. Burrows, T.J. Kemp, The photochemistry of the uranyl ion, *Chem. Soc. Rev.* 3 (1974) 139–165.
- [63] J.A. Kemlo, T.M. Shepherd, Quenching of excited singlet states by metal ions, *Chem. Phys. Lett.* 47 (1977) 158–162.